Available online at www.sciencedirect.com
ScienceDirect
Corrosion Science 49 (2007) 1918–1932
CORROSION SCIENCE
www.elsevier.com/locate/corsci

Steel corrosion in concrete: Determinist modeling of cathodic reaction as a function of water saturation degree

B. Huet [a,c], V. L'hostis [a,*], G. Santarini [b], D. Feron [a], H. Idrissi [c]

[a] *CEA Saclay, Département de Physico-Chimie, DEN/DANS/DPC, Bât. 158, 91191 Gif-sur-Yvette Cedex, France*
[b] *CEA Siège, Cabinet du Haut Commissaire, Bât. 447, 91191 Gif-sur-Yvette Cedex, France*
[c] *Laboratoire de Physico-Chimie Industrielle (LPCI), INSA de Lyon, Bât. Léonard de Vinci, 20 av. Albert Einstein 69621 Villeurbanne Cedex, France*

Received 8 May 2006; accepted 6 October 2006
Available online 28 November 2006

Abstract

The prediction of the long-term behavior of reinforced concrete structures involved in the nuclear waste storage requires the assessment and the modeling of the corrosion processes of steel reinforcement. This paper deals with the modeling of the cathodic reaction that is one of the main mechanisms of steel rebar corrosion. This model takes into account oxygen reduction and oxygen diffusion through a diffusion barrier (iron oxide and/or carbonated concrete) as a function of water saturation degree. It is demonstrated that corrosion rate of reinforcement embedded in concrete with water saturation degree as low as 0.9 could be under oxygen diffusion control. Thus, transport properties of concrete (aqueous and gaseous phase, dissolved species) are key parameters that must be taken into account to model electrochemical processes on the reinforcement.

Keywords: A. Kinetics; E. Modeling; C. Corrosion; D. Reinforcement; C. Long-term performance

* Corresponding author. Tel.: +33 1 69 08 32 13; fax: +33 1 69 08 84 41.
E-mail address: valerie.lhostis@cea.fr (V. L'hostis).

0010-938X/$ - see front matter © 2006 Elsevier Ltd. All rights reserved.
doi:10.1016/j.corsci.2006.10.005

1. Introduction

Reinforced concrete structures are largely used in the nuclear industry, including nuclear power plants and nuclear waste facilities. Steel reinforcement is used to improve the tensile strength of concrete structures, and more generally their mechanical resistance.

In nuclear waste storages, reinforced concrete structures have to provide not only improved mechanical properties but also the containment of nuclear wastes. Growth of cracks in concrete due to corrosion of rebars would alter its containment properties.

Non-alloyed or low-alloyed carbon steel is often used as reinforcement in these structures. Thanks to the high alkalinity of the concrete interstitial solution, reinforcement remains at a passive state. Very low corrosion rates are expected and no mechanical degradation should be generated. Nevertheless, concrete is a porous material that may react with the surrounded medium. Especially, the atmospheric carbon dioxide generates carbonation of concrete and leads to the alteration of its physical and chemical properties (pH decrease). Moreover, in carbonated concrete, the corrosion state of the rebars does no longer remain in its passive state and high corrosion rates can be observed. Growing of new iron oxides at the steel/concrete interface generates tensile stresses in the carbonated concrete that may lead to the cracking. Tuutti's diagram schematizes the time evolution of the steel/concrete interface [1] with the passive and active periods.

The aim of this study is to evaluate the duration of active corrosion period of reinforcements. More precisely, the authors plan to evaluate to what extent the cathodic reaction could be the rate-limiting step of the corrosion process during this active period. Concerning the oxygen reduction in degraded concrete, Raupach [2,3], proposes four environmental humidity scenarios that influences the global oxygen reduction rate: (1) constantly dry, (2) short-term wetting, (3) long-term wetting, (4) constantly water saturated. This classification corresponds to various water saturation profiles that consider only two different levels of water saturation, whether water saturated ($S_r = 1$) or non-water saturated ($S_r < 1$). As long as a thick concrete layer remains water saturated, then the corrosion rate is diffusion limited. Otherwise, in a non-water saturated concrete (HR $< 100\%$, i.e., $S_r < 1$) oxygen diffusion should never be the rate-limited step and is therefore neglected [2,3].

We propose in this paper an analytical study to evaluate the whole cathodic process as a function of the water saturation degree of the concrete, considering a continuous evolution of S_r with environmental relative humidity. The authors aim at answering the following question: should a determinist model of reinforcement corrosion take into account oxygen diffusion through degraded concrete even if water saturation degree is lower than 1 ($S_r < 1$)? In which range of S_r values the cathodic process is respectively under reaction control or under diffusion control?

2. Corrosion modeling: state of the art

Previous investigations on the electrochemical and on the corrosion behavior of iron immersed in alkaline solutions have highlighted very low oxidation kinetics [4–6]. The passive oxide layer remains very thin (several nanometers) [7] and cannot lead to the cracking of concrete. The chemical degradation of concrete (leading to high corrosion rate of the rebar) and the onset of high corrosion rate are therefore necessary conditions for cracking occurrence. The service life of a concrete structure is then determined (1) by the duration

of the ingress of aggressive species, (2) by the critical conditions required for the onset of active corrosion and (3) by the duration of the active corrosion period.

The chemical degradations of concrete due to chloride ingress or carbonation are well known. Moreover, the depassivation conditions in terms of chloride concentration or pH decrease have been subject to many investigations [8–11]. Thus, the time to depassivation may be predicted with an almost good accuracy.

A lot of experimental data are available on the corrosion rate of steel reinforcement in degraded (chloride polluted or carbonated) concrete. But to our knowledge no mechanistic modeling exists for reinforcement corrosion in carbonated concrete. Mechanistic models have been reported in the literature but most of them describe mild steel corrosion in other aqueous environments.

Three kinds of model are generally used to predict the long-term evolution of corrosion [12]: a material balance approach, a semi-empirical approach or a mechanistic modeling. However, only the mechanistic modeling allows a long-term prediction that cannot be reached with laboratory experiments.

The mechanistic models are based on the integration of elementary mechanisms in analytical or numerical models. Those models require the implementation of dissolution, diffusion and kinetic reaction constants, the latter constant being often not mentioned in the literature. The determinist laws deduced from these models may be then compared to semi-empirical laws evaluated from laboratory tests.

Few authors have tried to model iron corrosion in degraded concrete [13–15]. They propose to evaluate corrosion rate as a function of anodic polarization, cathodic polarization and electrical resistance of concrete. Each anodic and cathodic polarizations are evaluated with the Butler–Volmer activation law. This law permits the evaluation of corrosion rate as a function of the anodic and cathodic overpotentials and Tafel coefficient. Nevertheless, these models do take into account neither the chemical evolution in the oxide layer at the steel/concrete interface nor the aqueous transport of reactive species in the porosity of degraded concrete. Actually, the interfacial reaction kinetics may not be the controlling factor of the corrosion rate.

For instance, the corrosion modeling of mild steel in deep reductive clays is based on the physical description of the growing of a dense corrosion layer. In this particular case, the corrosion rate and the growing of the oxides layer is limited by species motion in the solid phase: electron or point default motion (anionic or cationic) [16,17].

In the case of atmospheric corrosion of low-alloyed steels, the wetting and drying cycles have been identified as critical parameters to evaluate the metal loss over time. In particular, the oxygen reduction during the wet period leads to high metal loss. The reduction of oxygen has been modeled assuming the electrical conductivity of the porous oxide layers. The transport of oxygen in a thin water layer on the iron oxides is the limiting step of this system [18,19].

3. Mechanistic modeling of corrosion in carbonated concrete

This section presents the basis of a new mechanistic model for rebar corrosion in carbonated concrete. The model is based on the analysis of ancient ferrous artifacts and laboratory experiments performed on mild steel immersed in carbonated solution [11]. Recent investigations on aged ferrous artefacts embedded in carbonated binders have shown a structuring of the oxides at the steel/concrete interface [20], this oxide being porous, even

in the vicinity of the iron substrate [21]. This structuring consists in a stratification of the iron oxides at the steel/concrete interface into two layers. The first layer is a "dense" product layer (DPL) consisting mainly in ferric oxy-hydroxide. The second layer called "transformed medium" (TM) consists in a precipitated ferric oxy-hydroxide in the porosity of concrete.

There are two kinds of rate-limiting steps: reaction kinetics or aqueous species transport. Each of these mechanisms is individually described in the following parts of the paper. Then the oxygen reduction rate is evaluated considering each mechanism.

3.1. Elementary steps

The corrosion process may be described by the elementary anodic (Eq. (1)) and cathodic (Eq. (2)) heterogeneous reactions of the overall corrosion process (Eq. (3)):

$$\frac{1}{2}O_2 + H_2O + 2e^- \Rightarrow 2OH^- \tag{1}$$

$$Fe \Rightarrow Fe^{2+} + 2e^- \tag{2}$$

$$H_2O + Fe + \frac{1}{2}O_2 \Rightarrow Fe^{2+} + 2OH^- \tag{3}$$

Considering that (1) the electrochemical partial reactions are irreversible, (2) the electrolyte is pH buffered and (3) the ferrous cation concentration remains constant, the corrosion rate depends only on oxygen concentration and on anodic and cathodic reaction kinetics.

In this work, we will consider that the anodic reaction kinetics is faster than the cathodic reaction kinetics. Moreover, we neglect the ohmic drop between anodic and cathodic area, assuming that the conductivity of porous media (iron oxide and/or carbonated concrete) remains high enough. In those conditions, the corrosion rate is controlled by the oxygen reduction.

3.1.1. Description of elementary steps

The iron oxide layer that covers the iron substrate is considered as porous. The oxygen reduction in a presence of a porous layer follows different elementary mechanisms, which are reported in Fig. 1. The iron oxide layer covering the substrate is assumed to be porous and allow species transport through gas or aqueous phase within the porosity. Oxygen reduction on iron compound embedded in porous media is then controlled by different elementary mechanisms. These mechanisms are reported in Fig. 1. So, oxygen is reduced locally, whether on the internal interface ($x = x_1$) or on the iron oxide surface developed within its volume. In the latter case, the iron oxide crystal is assumed to be an electroconductive solid. The only transport mechanism is supposed to be diffusion of oxygen (dissolved or gaseous).

3.1.2. Expression of concentrations in porous media

Various mathematical expressions of concentrations are introduced in order to apply Fick's laws to porous media. If the porous medium is a homogeneous medium, the relation between the oxygen concentrations, related to whether the interstitial solution volume or the total volume of the material (liquid, solid and gas), is expressed according to Eq. (4). This relation (Eq. (4)) can be extended to porous media that are not water saturated

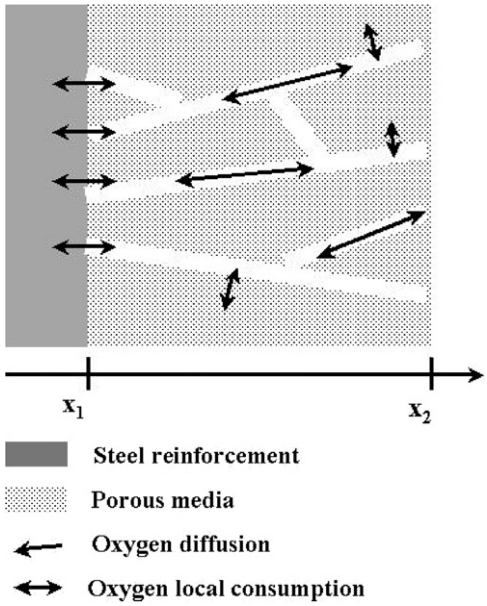

Fig. 1. Sketch of oxygen transport through a porous media and oxygen reduction. Porous layer is made of either a conductive iron oxide or of a non-conductive iron oxide or of a carbonated concrete.

(Eq. (5)), introducing the water saturation degree S_r (Eq. (7)). And in the same way, the oxygen concentration in gaseous phase (c_{g,O_2}) can be related to the total volume of the material (c_{mg,O_2}) as reported by Eq. (6):

$$C_{ml,O_2} = \phi_{water} C_{l,O_2} \tag{4}$$

$$c_{ml,O_2} = \phi S_r c_{l,O_2} \tag{5}$$

$$c_{mg,O_2} = \phi(1 - S_r) c_{g,O_2} \tag{6}$$

$$S_r = \frac{\phi_{water}}{\phi} \tag{7}$$

with

c_{ml,O_2} oxygen concentration in the liquid phase related to total material volume (mol/m^3),

c_{mg,O_2} oxygen concentration in the gaseous phase related to total material volume (mol/m^3),

c_{l,O_2} oxygen concentration in the liquid phase related to water volume (mol/m^3),

c_{g,O_2} oxygen concentration in the gaseous phase related to air volume (mol/m^3),

ϕ total porosity of porous media (%),

ϕ_{water} water saturated porosity (%),

S_r water saturation degree of porous media (%).

3.1.3. Pure interfacial reaction step

Oxygen reduction is assumed to be governed locally by a first order kinetics law. The oxygen reduction rate may be written as indicated in Eq. (8) where k is the kinetic constant

of the oxygen reduction ($\approx 10^{-5}$ m/s). We assume that only dissolved oxygen in interstitial solution may be reduced. At ambient temperature (25 °C), the kinetics of gaseous oxygen reduction is assumed to be far lower than the kinetics of dissolved oxygen reduction. Thus, whatever the water saturation degree is, the oxygen reduction depends only on the dissolved oxygen concentration at the interface as indicated by Eq. (9). However, the latter equation indicates that the effective kinetic constant of oxygen reduction ($k_{e,l}$) will depend on the water saturation degree S_r (Eq. (10)).

For specific conditions, it may be necessary to express the oxygen reduction kinetics (Eq. (8)) as a function of oxygen concentration in the gaseous phase (Eq. (12)). In those cases, we assume that the dissolved oxygen is in thermodynamic equilibrium with oxygen partial pressure (c_{v,O_2}) in the gaseous phase. Thus according to the Henry's law (Eq. (11)), Eq. (12)) is written.

Eqs. (10) and (13) indicate that the effective kinetic constant (K_e) of oxygen reduction in homogeneous porous media is strongly different, depending on which volume, gaseous, liquid or total, the oxygen concentration is related to

$$V(x) = k c_{ml,O_2}(x) \tag{8}$$

$$V(x) = k_{e,l} c_{l,O_2}(x) \tag{9}$$

$$k_{e,l} = k\phi S_r \tag{10}$$

$$c_{g,O_2} = \frac{K_H}{RT} c_{l,O_2} \tag{11}$$

$$V(x) = k_{e,g} c_{g,O_2}(x) \tag{12}$$

$$k_{e,g} = \frac{k\phi RTS_r}{K_H} \tag{13}$$

k kinetic constant of oxygen reduction ($\approx 10^{-5}$ m s^{-1}[22]),
$k_{e,l}$ effective kinetic constant of oxygen reduction: concentration related to the liquid phase volume (m s^{-1}),
$k_{e,g}$ effective kinetic constant of oxygen reduction: concentration related to the gaseous phase volume (m s^{-1}),
K_H Henry's dissolution constant of gaseous oxygen (7.47×10^4 Pa m^3 mol^{-1}),
R perfect gas constant (8.31 J mol^{-1} K^{-1}),
T temperature (K).

3.1.4. Pure diffusion step

The driving force of diffusion is the gradient of chemical potential. In the case of oxygen, the shift of chemical potential within porous concrete cover is only due to concentration variation, either in the gas phase or in the liquid phase. The first Fick's law expresses mathematically the diffusion mechanism in homogeneous media (here in one dimension, 1D). Moreover, there is a way to extend this formalism to porous media, in the case of species transport through the liquid phase (Eq. (14)) or gas phase (Eq. (15)).

The combination of the first Fick's law (Eq. (14)) with the mass balance equation, written for a representative volume of porous media, allows obtaining the second Fick's law (Eq. (16)). The latter equation may be solved after retaining only the oxygen concentration related to liquid phase volume (Eq. (17)). In the same way, the second Fick's law is written

for the transport of oxygen through the gas phase (Eq. (18)). The latter equations (17) and (18) indicate that the oxygen diffusion rate within the gas or liquid phase depends on the water saturation degree of the porous diffusion barrier:

$$j_{l,O_2} = -D_{e,l}\frac{\partial c_{l,O_2}}{\partial x} \tag{14}$$

$$j_{g,O_2} = -D_{e,g}\frac{\partial c_{g,O_2}}{\partial x} \tag{15}$$

$$\frac{\partial c_{ml,O_2}}{\partial t} = D_{e,l}\frac{\partial^2 c_{l,O_2}}{\partial x^2} \tag{16}$$

$$\frac{\partial c_{l,O_2}}{\partial t} = \frac{D_{e,l}}{\phi S_r}\frac{\partial^2 c_{l,O_2}}{\partial x^2} \tag{17}$$

$$\frac{\partial c_{g,O_2}}{\partial t} = \frac{D_{e,g}}{\phi(1-S_r)}\frac{\partial^2 c_{g,O_2}}{\partial x^2} \tag{18}$$

$$j_{O_2} = -D_e\frac{c_{O_2}(x_2) - c_{O_2}(x_1)}{X} = cst \tag{19}$$

j_{l,O_2} oxygen flux in liquid phase related to the surface of porous material (mol m^2 s^{-1}),
$D_{e,l}$ effective diffusion coefficient of species in the liquid phase of porous material (m^2 s^{-1}),
j_{g,O_2} oxygen flux in gaseous phase related to the surface of porous material (mol m^{-2} s^{-1}),
$D_{e,g}$ effective diffusion coefficient of species in the gaseous phase of porous material (m^2 s^{-1}).

The solution of the second order differential equation (Eqs. (17) and (18)) gives the oxygen concentration profile within the porous layer as a function of time for each initial and boundary conditions. In steady state, $\frac{\partial c}{\partial t} = 0$, the concentration profile remains linear and the oxygen flow is constant within the whole porous layer. This oxygen flow may be written as a function of oxygen concentration at the boundary of the porous layer $c_{O_2}(x_1)$ and $c_{O_2}(x_2)$ as well as its thickness (X), in the same manner for gaseous or dissolved oxygen (Eq. (19)).

3.1.5. Interfacial reaction and transport coupled step

An interfacial reaction and transport coupled step should be taken into account if oxygen diffuses through a conductive porous solid that is electronically connected to the reinforcement. The concrete barrier layer is assumed not to be a conductor of electricity. On the opposite, the newborn oxides may be electronically conductive (Fig. 2). For example, magnetite (Fe_3O_4) becomes conductive under low thermal activation, at room temperature (25 °C) [23]. In each homogenized elementary volume of the porous oxide layer, a part of oxygen diffuses (Eqs. (14) and (17)) and the other part is consumed at the iron oxide/interstitial solution interface (Eq. (20)), as drawn in Fig. 1. We assume that this mechanism may only take place if the oxide layer remains water saturated. Actually magnetite is not a stable phase in oxidative media generated by atmospheric conditions.

The local consumption of oxygen within the conductive oxide layer depends on the specific surface (related to the volume) developed locally ($s_a \cdot dx$) by the porous network, as indicated by equation (Eq. (20)). Eq. (21) allows converting the specific surface value

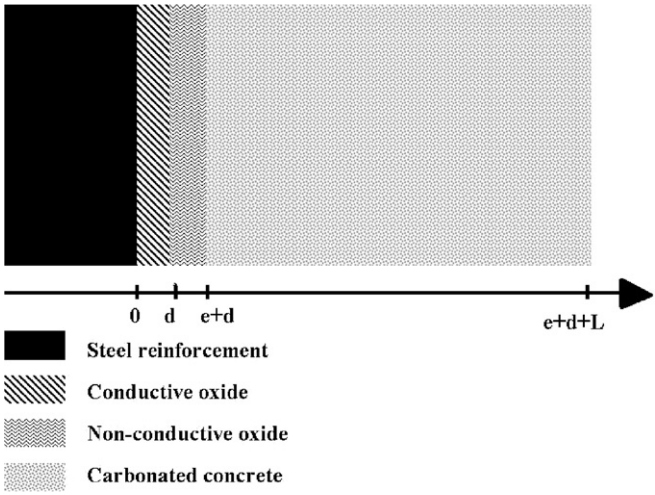

Fig. 2. Sketch of the system (corroded steel, carbonated concrete) during the active corrosion period.

(S_a, m^2/g) to the specific surface related to the total volume of the porous media (s_a, m^{-1}), considering a homogeneous porosity and density of the oxide layer.

The mass balance equation (or second Fick's law, Eq. (17)) is then corrected with a second term in its right member, as indicated by Eq. (22). This term expresses the local consumption of oxygen. In steady state, the simplified mass balance equation (Eq. (23)) is a second order differential equation, considering the variable λ (defined in Eq. (24)), which is homogeneous with a length. The resolution of Eq. (23), which is obtained in the case of a half finite diffusion layer, gives the oxygen concentration profile within the interstitial solution (Eq. (25)). This latter equation indicates obviously the exponential decrease of the concentration from the outer interface toward the reinforcement/conductive oxide interface. The hypothesis of half finite layer should not be ruled out as long as the value of λ is negligible compared to the oxide layer thickness. It means that the oxygen concentration should remain negligible at the steel/conductive oxide interface. Considering the following numerical application ($D_e = 10^{-12}\ m^2\ s^{-1}$, $s_a = 3.7\ 10^7\ m^{-1}$, $k = 10^{-5}\ m\ s^{-1}$ and $\phi = 0.1$), λ is evaluated to be about 1 μm. Thus, this model is valid in the presence of a conductive oxide layer with an accuracy better than 1% as long as its thickness is greater than 5λ, i.e., 5 μm.

$$V(x) = k s_a \phi c_{l,O_2}(x) \cdot dx \tag{20}$$

$$S_a = (1-\phi)\rho S_a \tag{21}$$

$$\frac{\partial c_{ml,O_2}}{\partial t} = D_{e,l}\frac{\partial^2 c_{l,O_2}}{\partial x^2} - k s_a \phi c_{l,O_2} \tag{22}$$

$$\lambda^2 \frac{\partial^2 c}{\partial x^2} - c = 0 \tag{23}$$

$$\lambda(\text{Eq. (23)}) \text{ is defined as:} \quad \lambda = \sqrt{\frac{D_{e,l}}{s_a k \phi}} \tag{24}$$

$$c_{l,O_2}(x) = c_{l,O_2}(x_2)\exp\frac{x - x_2}{\lambda} \tag{25}$$

ρ, iron oxide density (kg/m^3); S_a, specific surface of the iron oxide (m^2/g); s_a, specific surface related to the volume (3.7×10^7 m^{-1} [21]).

In a representative elementary cross-section (S as surface and dx as thickness), the elementary oxygen reduction current dI (Eq. (26)) is evaluated using the local rate of oxygen consumption (Eq. (20)) and Faraday's law. In Eq. (26), $s_a S \mathrm{d}x$ represents the local surface on which oxygen molecules are reduced. The integration of the elementary current dI on the whole conductive oxide layer thickness permits to calculate the global oxygen reduction current density i (Eq. (27)). However, the resolution of mass balance equation is only valid when $\lambda << (x_2 – x_1)$. Thus, Eq. (27) is simplified and gives Eq. (28). This equation is similar to Eq. (9). Only the effective kinetic constant is increased by a factor compared to the effective kinetic constant in the absence of a conductive oxide layer (Eq. (29)). Thus, whether a conductive oxide layer is connected to the reinforcement or not, the oxygen reduction rate will follow a first order kinetics law:

$$\mathrm{d}I = nFs_a k\phi c_{l,O_2}(x) \cdot S\mathrm{d}x \tag{26}$$

$$i = nFs_a k\lambda\phi c_{l,O_2}(x_2)\left[1 - \exp\left(-\frac{x_2 - x_1}{\lambda}\right)\right] \tag{27}$$

$$i = nFk_e c_{l,O_2}(x_2) \tag{28}$$

$$k_e = s_a \lambda k \phi \tag{29}$$

Finally, a simplified model of oxygen reduction does not need to take into account oxygen diffusion through an electronically conductive oxide layer. This model should just consider an increase of the effective kinetic constant, by a factor $s_a\lambda$, due to the presence of a conductive oxide layer.

3.2. Analysis of the rate-limiting step

From the definition and the expression of each of the three elementary mechanisms, one can evaluate the rate-limiting step of oxygen reduction. The true system, which is considered to describe oxygen reduction mechanism in the case of steel reinforcement embedded in carbonated concrete, consist in a multi layer system. Thus, one will consider (1) the mild steel reinforcement, (2) the porous oxide layer (d) that behaves like an electronic conductor and consists mainly of magnetite (Fe_3O_4), (3) a non-conductive iron oxide layer (e) that consist mainly of ferric oxi-hydroxide (lepidocrocite γ-FeOOH and/or goethite α-FeOOH), (4) the carbonated concrete thickness (L) with an adjustable water saturation degree S_r, and (5) the atmosphere that consists of an infinite stock of carbon dioxide and gaseous oxygen.

Case studies presented in literature do not always take into account of the presence of a conductive oxide layer at steel/carbonated concrete [20,24]. Thus, one should consider two cases, whether a conductive oxide layer is present or not. However, we demonstrate that both cases are very similar to each other if one considers only the oxygen reduction mechanism. In these conditions, oxygen diffuses first through carbonated concrete, then through a non-conductive oxide layer and finally oxygen is reduced whether on steel reinforcement or on the conductive oxide layer (Fig. 2).

Oxygen flux within the iron oxide layer and concrete cover are mathematically expressed, as indicated by Eqs. (30) and (31). It could be mentioned that these expressions are very similar to each other, no matter if dissolved or gaseous oxygen is concerned. The

dissolved oxygen consumption rate at the internal interface is expressed by Eq. (9) with $x = 0$. We demonstrated above the analogy between the oxygen reduction happening at steel reinforcement or inside the conductive oxide layer. Thus according to Eqs. (9), (12) and (28), oxygen reduction rate (V) on the internal interface is expressed by Eq. (32):

$$\text{(Flux within oxide layer) } j_{O_2,Ox_2} = -D_{e,Ox_2}\frac{c_{O_2}(d+e) - c_{O_2}(d)}{e} \tag{30}$$

$$\text{(Flux within concrete) } j_{O_2,Bet} = -D_{e,Bet}\frac{c_{O_2}(L+d+e) - c_{O_2}(d+e)}{L} \tag{31}$$

$$V = k_e c_{O_2}(0) \tag{32}$$

$$j_{O_2,Bet} = j_{O_2,Ox_2} = V \tag{33}$$

Those different elementary steps of the oxygen reduction process are connected in series. Thus, writing the mass balance equation for each zone and layer, and then for the whole system, one may establish, in steady state, an expression between the different flux (Eq. (33)). Finally, according to Eqs. (30)–(33), the oxygen reduction rate is written as a function of each elementary mechanism:

$$j_{O_2} = \frac{c_{O_2}}{\frac{1}{k_e} + \frac{e}{D_{e,Ox_2}} + \frac{L}{D_{e,bet}}} \tag{34}$$

The comparison of the terms of the denominator of Eq. (34) allows the determination of the rate-limiting step of oxygen reduction. We consider here that the only variables of the system are the water saturation degree and the thickness of the non-conductive oxide layer. Indeed, the thickness of the conductive oxide layer does not appear in Eq. (34). However one should remember that its thickness d should be greater than 5λ. Finally, the concrete cover L is constant.

There is lack of data in literature concerning diffusion properties (porosity, effective diffusion coefficient) and hydrous properties of iron oxide layers at steel/carbonated concrete interface. In this work, we consider the diffusion properties and hydrous properties of oxide(s) to be very similar to each other. Furthermore, the effective diffusion coefficient of oxygen in liquid or gaseous phase within iron oxide layers is supposed to be equal the one within carbonated concrete. Based on this assumption and considering the oxide layer thickness much lower than the concrete cover, Eq. (34) may be simplified to result in Eq. (35). The latter equation expresses the presence of only one diffusion barrier layer:

$$j_{O_2} = \frac{c_{O_2}}{\frac{1}{k_e} + \frac{L}{D_{e,Bet}}} \tag{35}$$

$$E_{crit} = \frac{D_{e,Bet}}{k_e} \tag{36}$$

If both terms of the denominator of Eq. (35) are equal to each other, one defines the value of the critical length E_{crit} (Eq. (36)) as the ratio of effective diffusion coefficient to effective kinetic constant. The value of this parameter depends only of the water saturation degree of concrete cover. The comparison of E_{crit} with concrete cover L allows to determine the type of kinetic control of oxygen reduction rate (Table 1). One should make this comparison for each water saturation degree of the porous diffusion barrier without neglecting the evolution of the effective kinetic constant and the effective diffusion coefficient with S_r.

Table 1
Various cases of rate-limiting step as a function of critical length and concrete cover

Condition	Denominator	Control
$L \prec\prec E_{crit}$	$\frac{1}{k_e} \succ\succ \frac{L}{D_{e,Bet}}$	Reaction
$L \approx E_{crit}$	$\frac{1}{k_e} \approx \frac{L}{D_{e,Bet}}$	Mixed
$L \succ\succ E_{crit}$	$\frac{L}{D_{e,Bet}} \succ\succ \frac{1}{k_e}$	Diffusion

Value of the denominator of Eq. (35).

According to experimental results of gas diffusion (hydrogen) in cement paste (Portland Cement CEM I, water to cement ratio 0.35), the value of effective diffusion coefficient of gaseous species $D_{e,v}$ increases from $10^{-13}\,m^2\,s^{-1}$ to $10^{-6}\,m^2\,s^{-1}$, with a decrease of the water saturation degree S_r from 1 to 0.5 [25] (Fig. 3). Moreover, it is worth noting that $D_{e,g}$ remains constant at low value around $1.0\times10^{-10}\,m^2\,s^{-1}$ in the S_r domain, from 0.9 to 0.95. These values can be used for the present analytical evaluation assuming that hydrogen and oxygen present the same behaviour in term of gaseous phase diffusion, and assuming that numerical results will be available for a cement paste.

On the opposite, the value of the effective kinetic constant is less dependent to S_r than the effective diffusion coefficient. As a matter of fact, k_e is proportional to S_r (Eqs. (10) and (13)): it means that the k_e values remain in the same order of magnitude whatever the S_r value is.

So, the evolution of E_{crit} with S_r follows the same trend as the one of effective diffusion coefficient. Using the experimental results of Sercombe et al. [25], the E_{crit} value is calculated for each value of S_r and compared to concrete cover (respectively dotted line and strikethrough zone, Fig. 4). We assume that the typical concrete cover ranges from 1 to 10 cm, depending on the type of reinforced structures. Moreover, the oxygen reduction rate is also evaluated according to Eq. (35) ($L = 1$, 3 or 10 cm).

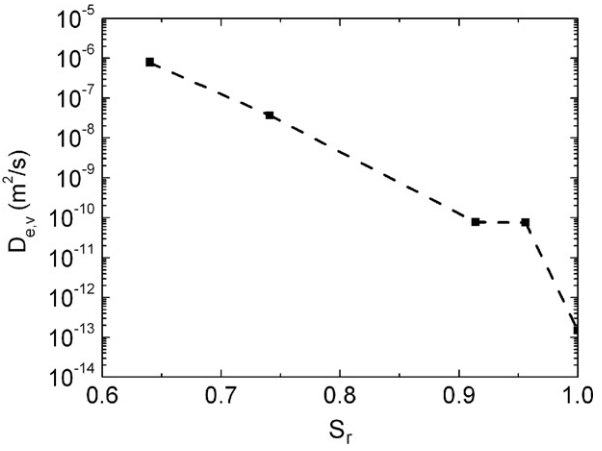

Fig. 3. Evolution of effective diffusion coefficient of hydrogen in gaseous phase as a function of water saturation degree S_r. Experimental results [25] obtained with hydrated Portland cement CEMI, water to cement ratio w/c = 0.35.

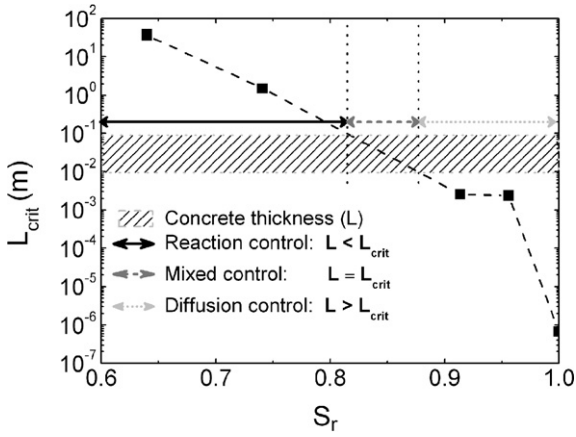

Fig. 4. Evolution of critical thickness as a function of water saturation degree S_r. Graphical assessment of the rate-limiting process.

As long the concrete cover remains water saturated ($S_r = 1$), the E_{crit} value is about 1 μm (Fig. 4), which is much lower than concrete cover. In that case, the rate-limiting step is oxygen diffusion (Table 1) through the concrete cover or even the non-conductive oxide layer, considering the latter is greater than 1 μm on long-term corroded samples [20]. In those conditions, the oxygen reduction rate is very low, between 6×10^{-5} and 6×10^{-4} μA cm^{-2} ($L = 10$ or 1 cm, respectively; Fig. 5). Considering these boundary conditions, it would take between 100 and 1000 years to form an oxide layer of 1 μm.

For water saturation degrees below ≈0.8, the E_{crit} value becomes much greater than the concrete cover and increases with the water desaturation of the porous cover. In these conditions ($S_r < 0.8$), the rate-limiting process is oxygen reduction (Table 1). However, in those conditions the corrosion rate is very high (≈200 μA cm^{-2}, Fig. 5), which is not

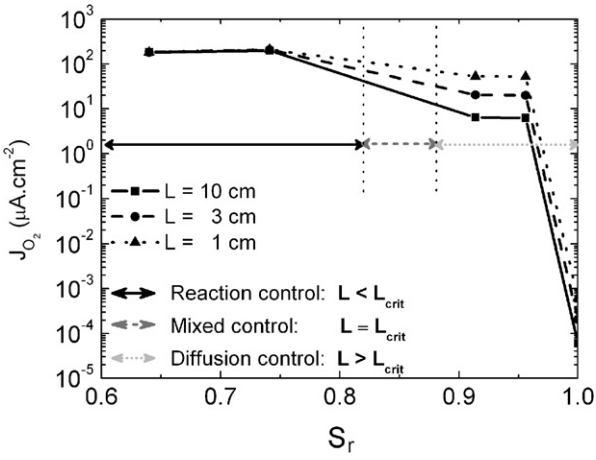

Fig. 5. Evaluation of oxygen reduction rates J_{O_2} as a function of the water saturation degree S_r for three concrete covers (1, 3 and 10 cm).

consistent with experimental results [1]. Thus the assumption of cathodic limitation of the corrosion process at low saturation degree ($S_r < 0.8$) is not relevant. Indeed, as proposed in literature [15], the rate-limiting mechanism at low S_r value is the anodic reaction.

In the intermediate ranges of S_r value ($S_r \in \{0.8; 0.9\}$), the E_{crit} value is in the same order of magnitude as the concrete cover (centimeter scale). Thus the oxygen reduction rate is under mixed reaction and transport control (Table 1): i.e., both mechanisms must be taken into account in order to evaluate the exact value. However, in this S_r range the calculated corrosion rates are high, between 10 and 100 μA cm^{-2} depending on S_r and geometry compared to data in literature by Tuutti [1], Alonso [26], Andrade [27] and Goni [28] who report typical corrosion rates between 1 and 10 μA cm^{-2} in that S_r range. Thus it is more likely, that the corrosion rate would be under mixed anodic and cathodic control in that S_r range, the cathodic reaction being itself under mixed reaction and transport control.

For water saturation degree greater than 0.9 (i.e., HR > 80% for this cement paste) but lower than 1, the E_{crit} value becomes smaller than the concrete cover. Thus the oxygen reduction rate is under diffusion control and depends therefore on the concrete thickness. Even under diffusion control of gaseous oxygen, the oxygen reduction rate remains high, between 6 and 50 μA cm^{-2} ($L = 1$ and 10 cm, respectively; Fig. 5) for the two S_r values, 0.9 and 0.95. Those results emphasize the critical role of water saturation degree on oxygen reduction rate, the latter decreasing by more than four orders of magnitude in the S_r range $\{0.95; 1\}$. Finally, the corrosion mechanism of reinforcement in good quality concrete could be under oxygen diffusion control, even at a water saturation degree of 0.9 (HR ≈ 80%).

4. Conclusion

This work aims at defining the rate-limiting mechanism of cathodic reaction during steel reinforcement corrosion and the S_r range of validity of cathodic reaction as rate-limiting process of the global corrosion process. Considering only the mechanisms of cathodic reaction, the reduction rate of oxygen is evaluated as a function of the water saturation degree (S_r) of the porous diffusion barrier layer. Numerical application of the analytical results introduced in this work indicates an evolution of the rate-limiting step as a function of S_r, for a cement paste (CEMI, w/c: 0.35):

- $S_r \in \{1.0; 0.9\}$: cathodic reaction is under diffusion control,
- $S_r \approx 0.9$: cathodic reaction is still under diffusion control, but oxygen diffusion rate is high enough to sustain reduction rates in the order of 10 μA cm^{-2},
- $S_r \in \{0.9; 0.8\}$: cathodic reaction is under mixed reaction and diffusion control,
- $S_r < 0.8$: cathodic reaction is under reaction control. Resistivity of the cementitious material has also to be taken into account.

Those results suggest the following conclusions concerning the overall issue of reinforcement corrosion modeling. The saturation degree of porous media and its diffusion properties are a key parameter to assess corrosion rates. Thus, it is of great importance to couple electrochemical reactions on the reinforcement to transport of species that plays a part in the electrochemical reactions, once active corrosion is initiated. This species transport include phase transport (aqueous and gas phase) and dissolved species transport

($O_{2,aq}$, Fe^{2+}, HCO_3^- and/or Cl^-) in concrete and the growing oxide layer. One should keep in mind that a section of water saturated concrete (here in 1D), whose thickness is greater than 1 μm, is wide enough to set the oxygen reduction rate under diffusion control and lead to low corrosion rate, whatever the location of this section is.

Acknowledgement

This study is part of the CIMETAL program of the Commissariat à l'Energie Atomique (CEA). It is financially supported by CEA, Electricité de France (EDF) and ANDRA.

References

[1] K. Tuutti, Corrosion of Steel in Concrete, Swedish Cement and Concrete Research Institute, 1982.
[2] M. Raupach, Investigations on the influence of oxygen on corrosion of steel in concrete – Part I, Mater. Struct. 29 (1996) 174–184.
[3] M. Raupach, Investigations on the influence of oxygen on corrosion of steel in concrete – Part II, Mater. Struct. 29 (1996) 226–232.
[4] D.D. MacDonald, B. Roberts, The cyclic voltammetry of carbon steel in concentrated sodium hydroxide solution, Electrochim. Acta 23 (1978) 781–786.
[5] R. Grauer, B. Knecht, P. Kreis, J.P. Simpson, Die Langzeit-Korrosiongeschwindigkeit des passiven Eisens in anaeroben alkalischen Lösungen, Werkstoffe Korros. 42 (1991) 637–642.
[6] S. Joiret, M. Keddam, Use of EIS, ring-disk electrode, EQCM and Raman spectroscopy to study the film of oxides formed on iron in 1 M NaOH, Cem. Concr. Res. 24 (2002) 7–15.
[7] P. Schmuki, M. Büchler, H. Böhni, et al., Passivity of Iron in alkaline solutions studied by in situ XANES and a Laser reflection technique, J. Electrochem. Soc. 146 (1999) 2097–2102.
[8] W. Breit, Kritischer Chloridegehalt-Untersuchungen an Stahl in chloridhaltigen alkalischen Lösungen, Mater. Corros. 49 (1998) 539–550.
[9] C. Alonso, M. Castellote, C. Andrade, Chloride threshold dependence of pitting potential of reinforcements, Electrochim. Acta 47 (2002) 3469–3481.
[10] M.A. Climent, C. Gutiérrez, Proof by UV–visible modulated reflectance spectroscopy of the breakdown by carbonation of the passivating layer on iron in alkaline solution, Surf. Sci. 330 (1995) 651–656.
[11] B. Huet, V. L'Hostis, F. Miserque, H. Idrissi, Electrochemical behavior of mild steel in concrete: Influence of pH and carbonate content of concrete pore solution, Electrochim. Acta 51 (2005) 172–180.
[12] ANDRA, Référentiel matériaux, Ed. ANDRA, November 2001.
[13] I. Petre-Lazar, Evaluation du comportement en service des ouvrages en béton armé soumis à la corrosion des aciers – Outil d'aide à la décision, Thesis of University of Laval, 2000.
[14] Z.P. Bažant, Physical model for steel corrosion in concrete sea structures – application, J. Struct. Div. (1979) 1155–1166.
[15] F. Hunkeler, Monitoring of repaired reinforced concrete structure by means of resistivity measurements, Mater. Sci. Forum 247 (1997) 93–106.
[16] C. Bataillon, Application of the Point Defect Model to modeling the corrosion of iron based canisters in geological repository, in: International Workshop Prediction of Long Term Corrosion Behaviour in Nuclear Waste Systems, Cadarache, 26–29 November 2001.
[17] D.D. MacDonald, The point defect model for the passive state, J. Electrochem. Soc. 139 (1992) 3434–3449.
[18] S. Hoerlé, F. Mazaudier, Ph. Dillmann, G. Santarini, Advances in understanding atmospheric corrosion of iron. II. Mechanistic modeling of wet–dry cycles, Corros. Sci. 46 (2004) 1431–1465.
[19] M. Stratmann, J. Müller, The mechanism of the oxygen reduction on rust covered metal substrates, Corros. Sci. 36 (1994) 327–359.
[20] W.J. Chitty, P. Dillmann, V. L'Hostis, C. Lombard, Long-term corrosion resistance of metallic reinforcements in concrete – a study of corrosion mechanisms based on archaeological artefacts, Corros. Sci. 47 (2005) 1555–1581.
[21] Ph. Dillmann, F. Mazaudier, S. Hœrlé, Advances in understanding atmospheric corrosion of iron. I. Rust characterization of ancient ferrous artefact exposed to indoor atmospheric corrosion, Corros. Sci. 46 (2004) 1401–1429.

[22] A.J. Bard, L.R. Faulkner, Electrochemical Methods: Fundamentals and Applications, Wiley, New York, 1980.
[23] R.M. Cornell, U. Schwertmann, The Iron Oxides, Wiley VCH, 2003, ISBN 3-527-30274-3, 664 p.
[24] G.S. Duffó, W. Morris, I. Raspini, C. Saragovi, A study of steel rebars embedded in concrete during 65 years, Corros. Sci. 46 (2004) 2143–2157.
[25] J. Sercombe R. Vidal, F. Adenot, Diffusion des gaz dans les ciments: mécanismes et paramètres principaux, in: French Symposium Transfert 2006, Lille, 1–2 February 2006.
[26] C. Alonso, C. Andrade, J.A. González, Relation between resistivity and corrosion rate of reinforcements in carbonated mortar made with several cement types, Cem. Concr. Res. 18 (1988) 687–698.
[27] C. Andrade, C. Alonso, J. Sarría, Corrosion rate evolution in concrete exposed to the atmosphere, Cem. Concr. Composites 24 (2002) 55–64.
[28] S. Goñi, C. Alonso, C. Andrade, Relationship between resistivity, porosity and corrosion rate of rebars in concrete, in: Proceedings of the European Symposium: Corrosion and Deterioration of Buildings, CSTB-CEFRACOR, 13–16 November 1990.